Chemical mechanism of inorganic oxidants in the TiO2/UV process: Increased rates of degradation of chlorinated hydrocarbons

ARTICLE *in* ENVIRONMENTAL SCIENCE AND TECHNOLOGY · OCTOBER 1995

Impact Factor: 5.33 · DOI: 10.1021/es00010a017 · Source: PubMed

3 AUTHORS, INCLUDING:

Michael R. Hoffmann
California Institute of Technology
379 PUBLICATIONS **30,162** CITATIONS

Environ. Sci. Technol. 1995, 29, 2567–2573

Chemical Mechanism of Inorganic Oxidants in the TiO_2/UV Process: Increased Rates of Degradation of Chlorinated Hydrocarbons

SCOT T. MARTIN, ALBERT T. LEE, AND MICHAEL R. HOFFMANN*

W. M. Keck Laboratories, California Institute of Technology, Pasadena, California 91125

Particulate suspensions of TiO_2 irradiated with UV light at wavelengths shorter than 385 nm catalyze the autooxidation of chlorinated hydrocarbons such as 4-chlorophenol (4-CP). The addition of oxyanion oxidants such as ClO_2^-, ClO_3^-, IO_4^-, $S_2O_8^{2-}$, and BrO_3^- increases the rate of photodegradation of 4-CP in the following order: $ClO_2^- > IO_4^- > BrO_3^- > ClO_3^-$. In the absence of TiO_2, ClO_3^- shows no photoreactivity toward 4-CP, while HSO_5^- and MnO_4^- exhibit rapid thermal reactivity with 4-CP. BrO_3^- appears to increase photoreactivity by scavenging conduction-band electrons and reducing charge-carrier recombination. With ClO_3^- as an oxidant, the degradation of 4-CP appears to follow three concurrent pathways. Kinetic equations for the rate of degradation of 4-CP as a function of [4-CP], [ClO_3^-], and [O_2] and of the light intensity are derived from a proposed mechanism.

Introduction

Under normal conditions, TiO_2 catalyzes the oxidation of chlorinated hydrocarbons in the presence of UV radiation at photon energies equal to or greater than the band-gap energy of 3.2 eV (λ = 385 nm) according to the following stoichiometry (*1*):

$$C_xH_yCl_z + \left(x + \frac{y-z}{4}\right)O_2 \xrightarrow[h\nu,\ TiO_2]{} xCO_2 + zH^+ + zCl^- + \left(\frac{y-z}{2}\right)H_2O \quad (1)$$

The addition of inorganic oxidants such as HSO_5^-, ClO_3^-, IO_4^-, and BrO_3^- increases the rate of degradation of chlorinated hydrocarbons in slurries of TiO_2 irradiated with ultraviolet light (*2–5*). The oxidants are proposed to increase quantum efficiencies partially by inhibiting electron-hole pair recombination through scavenging conduction-band electrons at the surface of TiO_2 and partially by augmenting the TiO_2/UV process through thermal and photochemical oxidations in the bulk solution. However, mechanistic studies on the role of the oxyanions in the TiO_2/UV process have not previously been carried out.

In this paper, we attempt to elucidate the detailed mechanism by which oxyanion oxidants serve as efficient electron acceptors in TiO_2/UV oxidations. In this regard, we have studied the photooxidation of 4-chlorophenol (4-CP) in suspensions of Degussa P25. The choice of electron-donating substrate and photocatalyst was made because they have been widely studied previously (*6–8*) and are considered a standard reaction system for the evaluation of the TiO_2/UV process (*9–11*).

Experimental Section

Photoreactivity Studies. Irradiations were performed with a 1000-W Xe arc lamp (Oriel Corp.) at 25 °C according to previously described procedures (*12–14*). Neutral density filters (Oriel) were used to adjust the light intensity, which was found to be 2.1 mEinstein min^{-1} without attenuation. A bandpass filter (Corning 7-60-1, 320 < λ < 380 nm) was used during the actinometry to avoid bleaching of Aberchrome 540.

Aqueous slurries (24 mL) of TiO_2 (1.0 g/L), 4-chlorophenol (100 μM), or KI (1 mM) and a particular oxidant (typically 100 mM) were prepared. The stirred aqueous slurries were bubbled with humid O_2 or N_2 (10 mL min^{-1}) for 90 min prior to and (for 4-CP only) during the irradiation to maintain oxygenated or deoxygenated conditions, as appropriate. The sparging of the KI slurry was followed by the introduction of a static Ar atmosphere under positive pressure, which prevented the volatilization of I_2 during the irradiation and excluded O_2 from the system. At periodic time intervals, aliquots (100 μL) of the slurry were extracted through 0.45-μm syringe filters. Nylon filters (Nalgene) were used for organic analysis, and Teflon filters (Gelman) were used for I_3^- analysis.

Analysis. Separation and quantification of organic intermediates was accomplished by HPLC (Hewlett Packard Series II 1090 liquid chromatograph). Compounds were separated on a reverse-phase column (Hewlett-Packard 5-μm ODS Hypersil) using a gradient elution program (100% H_3PO_4 buffer (pH 3.0) to 80:20 H_3PO_4/CH_3CN). Diode array detection at 224 and 280 nm was used for quantification. Production of I_3^- was quantified spectrophotometrically (HP 8452A) using ϵ(352 nm) = 26 400 M^{-1} cm^{-1} (*15*).

Results

The time series data of the photooxidation experiments (i.e., 4-CP concentration versus irradiation time) typically consist of five data points and are reduced by calculating apparent quantum efficiencies, Φ, as follows: $\Phi = |d[4CP]/dt|/I_{incident}$ where $d[4CP]/dt$ is the initial rate of disappearance of 4-CP and $I_{incident}$ is the incident light intensity determined by chemical actinometry. The apparent quantum efficiencies for the TiO_2/UV photooxidation of 4-CP in the presence of several oxidants are shown in Table 1. For irradiation in the absence of TiO_2, Φ decreases in the order $ClO_2^- > IO_4^- > BrO_3^- > ClO_3^-$. Of these, only ClO_3^- shows no direct photoreactivity with respect to 4-CP oxidation. ClO_2^-, IO_4^-, BrO_3^-, and ClO_3^- exhibit negligible dark reactivity at these concentrations whereas 0.1 M HSO_5^- and MnO_4^- are highly reactive in the absence of irradiation. In the presence of TiO_2, Φ increases and follows the same relative order of $ClO_2^- \sim IO_4^- > BrO_3^- > ClO_3^-$ over a pH range of 3–6.

* To whom correspondence should be addressed.

0013-936X/95/0929-2567$09.00/0

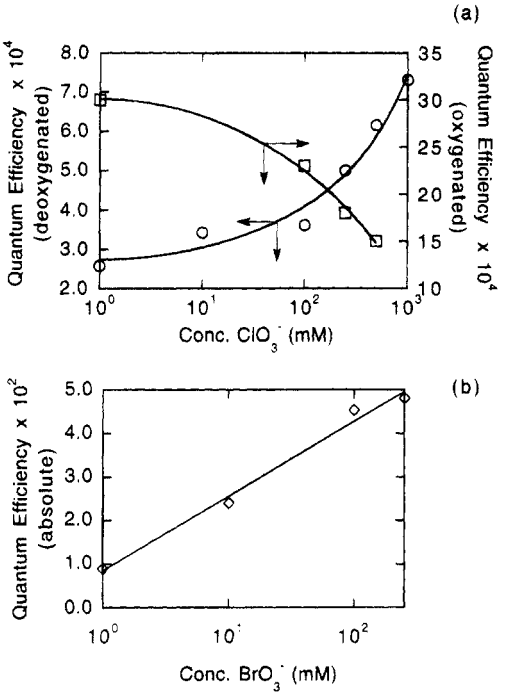

FIGURE 1. (a) Initial quantum efficiencies for the photooxidation of 4-CP in deoxygenated (○) and oxygenated (□) TiO_2 slurries as a function of log [ClO_3^-]. (b) Initial quantum efficiencies for the photooxidation of 4-CP (◇) as a function of log [BrO_3^-]. O_2 has no apparent effect. Conditions: See Table 1.

Increasing the concentration of ClO_3^- from 10^{-3} to 1 M yields higher Φ values in deoxygenated slurries (Figure 1a, ○). No saturation effect is observed up to 1 M ClO_3^-. However, a minimum concentration of 10 mM ClO_3^- is necessary for a noticeable increase in Φ. The Φ values in the presence of ≤1 mM ClO_3^-, N_2 alone (i.e., 0 mM ClO_3^-), 0.1 M Cl^-, and 0.1 M ClO_4^- are essentially the same within experimental error (i.e., $\Phi(\times 10^4) = 2.6$). Hydroquinone and benzoquinone are the principal intermediates detected by HPLC. Ion chromatographic measurements indicate ClO_3^- is reduced to Cl^- stoichiometrically with the loss of 4-CP; steady-state intermediates such as $HClO_2$ ($pK_a = 2$) or HOCl ($pK_a = 7.5$) are not detected.

In contrast to the deoxygenated slurries, increasing concentrations of ClO_3^- in the presence of oxygen yield lower Φ values (Figure 1a, □). However, Φ_{min} in the presence of oxygen (i.e., $\Phi(\times 10^4) = 15$ for 0.5 M ClO_3^-) is 2.0 times greater than Φ_{max} in the absence of oxygen (i.e., $\Phi(\times 10^4) = 7.5$ for 1 M ClO_3^-).

In the absence of TiO_2 and dioxygen, a homogeneous photoreaction occurs between BrO_3^- and 4-CP (data not shown). The Φ values increase steadily with [BrO_3^-] from 1 to 250 mM. The addition of O_2 has no apparent effect. The maximum Φ value due to homogeneous photoreactions, Φ_{homo}, is 0.13×10^{-2} for the range of concentrations studied. In the presence of TiO_2, both heterogeneous and homogeneous photoreactions occur (Figure 1b, ◇). The smallest Φ value, Φ_{hetero}, is 1.0×10^{-2}. Because $\Phi_{hetero} \gg \Phi_{homo}$ under our experimental conditions, we conclude that homogeneous photoreactions are negligible to a first approximation in the discussion of the mechanism of BrO_3^- in heterogeneous photooxidations. The addition of O_2 to the TiO_2/BrO_3^- suspension has no apparent effect under our experimental conditions.

Higher quantum efficiencies are often observed at lower incident light intensities due to decreased charge-carrier

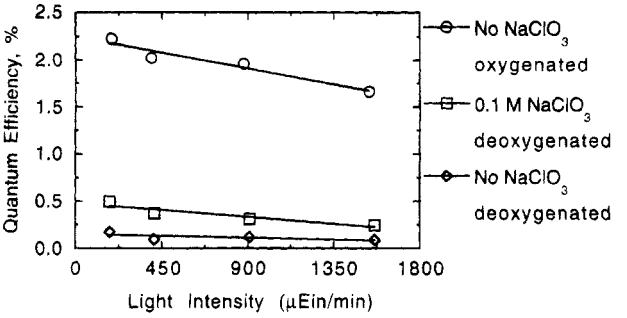

FIGURE 2. Quantum efficiency for the disappearance of 4-CP in a slurry of $NaClO_3$, O_2, and TiO_2 as a function of incident light intensity. Conditions: See Table 1.

Quantum efficiency	△ No $NaClO_3$ oxygenated	□ $NaClO_3$ oxygenated	○ No $NaClO_3$ deoxygenated	◇ $NaClO_3$ deoxygenated	× $NaClO_3$ wo/P25 deoxygenated
$\Phi_i \times 10^4$	7.6	6.3	4.3	4.3	0.0
$\Phi_{ss} \times 10^5$	1.6	1.1	1.1	0.7	0.0

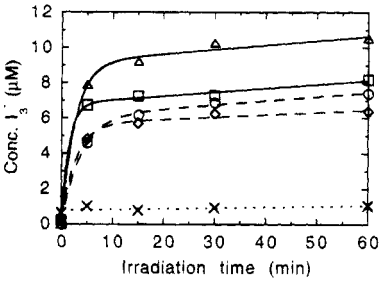

FIGURE 3. Formation of I_3^- in suspensions of 1 mM I^-, 0.1 M ClO_3^-, O_2, and TiO_2 irradiated with UV light. Initial (i) and steady-state (ss) quantum efficiencies are shown in the legend. Conditions: See Table 1.

recombination rates (*12, 13*). The effect of light intensities on Φ follows this trend (Figure 2). The slope $|\partial\Phi/\partial I|$ follows the order: {no ClO_3^-, O_2} > {0.1 M ClO_3^-, no O_2} > {no ClO_3^-, no O_2} where I is the light intensity.

The heterogeneous oxidation of I^- to I_3^- catalyzed by TiO_2 has been studied previously (*15–19*). In this study, we also investigated the formation of I_3^- by TiO_2/UV in the presence of ClO_3^- and/or O_2 as shown in Figure 3. In the absence of TiO_2, no I_3^- is formed. In the presence of TiO_2, an initial rapid formation of I_3^- from the oxidation of I^- is followed by a continuous slow formation according to the order: {no ClO_3^-, O_2} > {0.1 M ClO_3^-, O_2} > {no ClO_3^-, no O_2} ~ {0.1 M ClO_3^-, no O_2}. In addition, the yield of I_3^- in the oxygenated slurry is decreased by the addition of ClO_3^- as was seen in the case of 4-CP. However, unlike the 4-CP experiments, the initial rate of I_3^- formation in deoxygenated slurries is independent of the presence of ClO_3^-.

Discussion

The quantum efficiencies obtained for the degradation of 4-CP under a set of consistent experimental conditions (I = 2.1 mEinstein min^{-1}, $\lambda > 340$ nm, deoxygenated, [TiO_2] = 1 g/L, pH unadjusted, T = 25 °C, $[4\text{-CP}]_0$ = 100 μM) are given in Table 1. UV absorption by BrO_3^-, IO_4^-, and ClO_2^- results in direct photochemistry. Dark oxidation proceeds rapidly at 25 °C only for HSO_5^- and MnO_4^-, though all of the oxidants are thermodynamically capable of degrading 4-CP (E° = 0.80 V vs NHE) (*6, 20*). The absence of photochemistry and dark chemistry in a solution of ClO_3^- and 4-CP suggested that ClO_3^- was the appropriate

TABLE 1

Apparent Quantum Efficiencies ($\Phi \times 10^2$) for the Photooxidation of 4-CP by the TiO_2/UV Process in the Presence of Several Oxidants (0.1 M $NaClO_3$, 0.1 M $KBrO_3$, 18 mM KIO_4, 0.1 M $NaClO_2$, and 1 atm O_2)[a]

	quantum efficiency	
oxyanion oxidant	without TiO_2	with TiO_2
ClO_3^-	0.0	0.03
BrO_3^-	0.03	4.6
IO_4^-	0.9	4.8
ClO_2^-	2.2	4.8
O_2	0.0	0.3

[a] Conditions: I = 2.1 mEinstein min^{-1}, $\lambda > 340$ nm, deoxygenated, $[TiO_2]$ = 1 g/L, pH unadjusted, T = 25 °C, $[4\text{-CP}]_0$ = 100 μM.

inorganic oxidant for initial mechanistic studies. Although ClO_3^- degrades 4-CP more slowly (Table 1) than the other oxyanions, complications in the interpretation of our results were avoided because parallel reaction pathways are not available (cf. IO_4^-/4-CP/hν and IO_4^-/4-CP/hν/TiO_2). In addition, the mechanism of BrO_3^- is also studied because the quantum efficiency (Table 1) is relatively high and the ratio between the heterogeneous and homogeneous photoreactivities (Φ_{hetero}:$\Phi_{homo} \gg 1$) is large enough that the effects of the latter may be assumed to be negligible.

Conduction-Band Electron Scavengers. The positive monotonic relationship seen in Figure 1a (○) and b (◇) between the Φ values and the concentrations of ClO_3^- and BrO_3^- in deoxygenated TiO_2 suspensions supports the hypothesis that the oxyanions scavenge conduction-band electrons, reduce charge-pair recombination, and promote the oxidation of 4-CP by valence-band holes. The relevant reduction potentials are as follows (*21, 22*):

$$ClO_3^- + 2H^+ + e^- \rightarrow ClO_2 + H_2O \qquad E^\circ = 1.15\ V \quad (2)$$

$$ClO_3^- + 6H^+ + 6e^- \rightarrow [ClO_2^-, HOCl] \rightarrow Cl^- + 3H_2O \qquad E^\circ = 1.44\ V \quad (3)$$

$$BrO_3^- + 2H^+ + e^- \rightarrow BrO_2\ H_2O \qquad E^\circ = 1.15\ V \quad (4)$$

$$BrO_3^- + 6H^+ + 6e^- \rightarrow [BrO_2^-, HOBr] \rightarrow Br^- + 3H_2O \qquad E^\circ = 1.44\ V \quad (5)$$

According to this hypothesis, an additional electron scavenger such as O_2 should further reduce charge-pair recombination and thus increase the rate of 4-CP degradation. In fact, even at the lowest BrO_3^- concentrations (1 mM), O_2 has no apparent effect on the observed rates of degradation (Figure 1b). The negligible effect of O_2 suggests BrO_3^- scavenges conduction-band electrons more efficiently than O_2.

ClO_3^-, on the other hand, reduces photoreactivity in the presence of O_2 (Figure 1a, □). Further experimental evidence is also inconsistent with the scavenging of conduction-band electrons by ClO_3^-: continuous production of Cl^- ions should occur in conjunction with the valence-band hole oxidation of water (*23–27*). In fact, Cl^- ions are produced in an approximate stoichiometric relationship to the 4-CP degraded (corrected for Cl^- liberated from 4-CP).

Radical Scavengers. The negative correlation between $[ClO_3^-]$ and the Φ values (Figure 1a, □) suggests ClO_3^- may scavenge active radical species that are generated in oxygenated slurries. The initial reductive event on TiO_2 is believed to be the formation of superoxide ion followed by the subsequent formation of active oxygen species, which contribute to the oxidation of 4-CP (*2, 28*):

$$O_2 + e^-_{cb} \rightarrow O_2^- \rightarrow \rightarrow \rightarrow O_2^-, HOO, HOOH, HOO^-, HO \quad (6)$$

Scavenging of the active oxygen species by ClO_3^- should have the net effect of reducing photoreactivity. However, this possibility does not appear plausible due to apparent kinetic limitations (*29, 30*) in the known generation pathways of ClO_3 ($E^\circ(ClO_3/ClO_3^-) \approx 2.1$ V) (*31*):

$$^\bullet OH + ClO_3^- \rightarrow OH^-\ ClO_3^\bullet \qquad k < 1 \times 10^6\ M^{-1}\ s^{-1} \quad (7)$$

$$O_2^- + ClO_3^- \rightarrow \text{products} \qquad k < 0.003\ M^{-1}\ s^{-1} \quad (8)$$

Mills et al. (*10*) determined that the photooxidation of 4-CP is best described by three parallel reaction pathways. One reaction pathway leads to an unstable intermediate that undergoes ring cleavage and subsequent rapid decarboxylation and dechlorination. The other two reaction pathways result in stable intermediates, including hydroquinone (HQ) and 4-chlorocatechol (4-CC). Consistent with this explanation and other previous mechanistic studies (*4, 32–35*), we propose the reactions in Table 2 and Figure 4 to explain the effects of ClO_3^- and the formation of the observed reaction intermediates. The apparent reaction order for $[ClO_3^-]$ is between 0.1 and 0.4, as calculated by the method of initial rates for the data in Figure 1. A fractional reaction order is consistent with the concurrent free-radical pathways (*36*).

Reaction Mechanism. In the mechanism shown in Figure 4, 4-CP reacts with $^\bullet OH$ to form the 4-chlorodihydroxycyclodienyl radical (4-CD). After this initial hydroxylation, three parallel reaction pathways appear to be open. One pathway involves the reduction of 4-CD by a conduction-band electron to yield HQ and Cl^-. In the second pathway, 4-CD reacts with dioxygen to form the molecule 4-CDO. In the third pathway, the abstraction of an electron from 4-CD to yield 4-CD^+ is facilitated by ClO_3^-. 4-CD^+ is stabilized by a resonance interaction and by the strong electron-releasing capability of the ^-OH substituent at the 1-position (*37*). The reactive intermediates 4-CDO and 4-CD^+ undergo further photo and thermal reactions subsequent to their formation. Based on this mechanism, the reaction intermediates should be different depending upon the pathway that is dominant under a given set of experimental conditions. Previous work has shown that ClO_3^- affects the product mix obtained from the photooxidation of atrazine by the TiO_2/UV process (*2*).

Kinetic Description. Our goal is to express Φ as a function of $[O_2]$, $[ClO_3^-]$, and [4-CP] based on the chemical reactions and kinetic equations shown in Table 2. The notation is as follows: ≡ indicates a surficial group, $[\equiv X]$ is the surface concentration of species X (mol L^{-1}), e^- is a conduction-band electron, $\equiv e^-$ is a surficial electron (e.g., ≡Ti(III)), h^+ is a valence-band hole, $\equiv h^+$ is a surficial hole (e.g., $\equiv TiOH^{\bullet+}$), $\equiv O_2$ is adsorbed dioxygen (e.g., ≡Ti(IV)-

TABLE 2

Chemical Reactions and Kinetic Equations of Proposed Mechanism for TiO_2/UV Photooxidation of 4-CP in the Presence of O_2 and ClO_3^-

Chemical Reactions

k_1 $\equiv$4-CP + $\equiv h^+ \rightarrow \equiv$4-CD (T2.1)

k_{-1}: $\equiv$4-CD + $\equiv e^- \rightarrow \equiv$4-CP (T2.2)

k_2: $\equiv$4-CD + $\equiv ClO_3^- \rightarrow$ 4-CD^+ (T2.3)

k_3: $\equiv$4-CD + $\equiv O_2 \rightarrow \rightarrow$ pdts (T2.4)

k_4: $\equiv e^- + \equiv h^+ \rightarrow TiO_2$ (T2.5)

k_5: $TiO_2 + h\nu \rightarrow e^- + h^+$ (T2.6)

k_6: $e^- \rightarrow \equiv e^-$ (T2.7)

k_7: $h^+ \rightarrow \equiv h^+$ (T2.8)

k_8: $\equiv e^- + \equiv O_2 \rightarrow \equiv O_2^-$ (T2.9)

Surface Adsorption

$$K_1 = \frac{[\equiv O_2]}{[O_2][\equiv \text{Ti(IV)}]} \quad \text{(T2.10)}$$

$$K_2 = \frac{[\equiv ClO_3^-]}{[ClO_3^-][\equiv \text{Ti(IV)}]} \quad \text{(T2.11)}$$

$$K_3 = \frac{[\equiv 4CP]}{[4CP][\equiv \text{Ti(IV)}]} \quad \text{(T2.12)}$$

Surface Coverage

$$\Gamma_1{:}[\equiv O_2] = \frac{K_1[O_2][\equiv \text{Ti(IV)}]_0}{1 + K_1[O_2] + K_2[ClO_3^-] + K_3[4CP]} \quad \text{(T2.13)}$$

$$\Gamma_2{:}[\equiv ClO_3^-] = \frac{K_2[ClO_3^-][\equiv \text{Ti(IV)}]_0}{1 + K_1[O_2] + K_2[ClO_3^-] + K_3[4CP]} \quad \text{(T2.14)}$$

$$\Gamma_3{:}[\equiv 4\text{-CP}] = \frac{K_3[4CP][\equiv \text{Ti(IV)}]_0}{1 + K_1[O_2] + K_2[ClO_3^-] + K_3[4CP]} \quad \text{(T2.15)}$$

Kinetic Equations

$$\frac{d[4CP]}{dt} = -k_1[\equiv h^+][\equiv 4\text{-CP}] + k_{-1}[\equiv e^-][\equiv 4\text{-CD}] \quad \text{(T2.16)}$$

$$\frac{d[4CD]}{dt} = +k_1[\equiv h^+][\equiv 4\text{-CP}] - k_{-1}[\equiv e^-][\equiv 4\text{-CD}] - k_2[\equiv 4\text{-CD}][\equiv ClO_3^-] - k_3[\equiv 4\text{-CD}][\equiv O_2] \quad \text{(T2.17)}$$

$$\frac{d[\equiv e^-]}{dt} = k_6[e^-] - k_4[\equiv e^-][\equiv h^+] - k_8[\equiv e^-][\equiv O_2] - k_{-1}[\equiv e^-][\equiv 4\text{-CD}] \quad \text{(T2.18)}$$

$$\frac{d[\equiv h^+]}{dt} = k_7[h^+] - k_4[\equiv e^-][\equiv h^+] - k_1[\equiv h^+][\equiv 4\text{-CP}] \quad \text{(T2.19)}$$

$$\frac{d[e^-]}{dt} = k_5 - k_6[e^-] \quad \text{(T2.20)}$$

$$\frac{d[h^+]}{dt} = k_5 - k_7[h^+] \quad \text{(T2.21)}$$

Steady-State Approximation

$$\frac{d[4CD]}{dt} = \frac{d[\equiv e^-]}{dt} = \frac{d[\equiv h^+]}{dt} = \frac{d[e^-]}{dt} = \frac{d[h^+]}{dt} = 0 \quad \text{(T2.22)}$$

Charge-Neutrality

$$[\equiv e^-] + [e^-] - [\equiv h^+] - [h^+] = 0 \quad \text{(T2.23)}$$

Relative Reaction Rates

$$k_3 > k_2 \quad \text{(T2.24)}$$

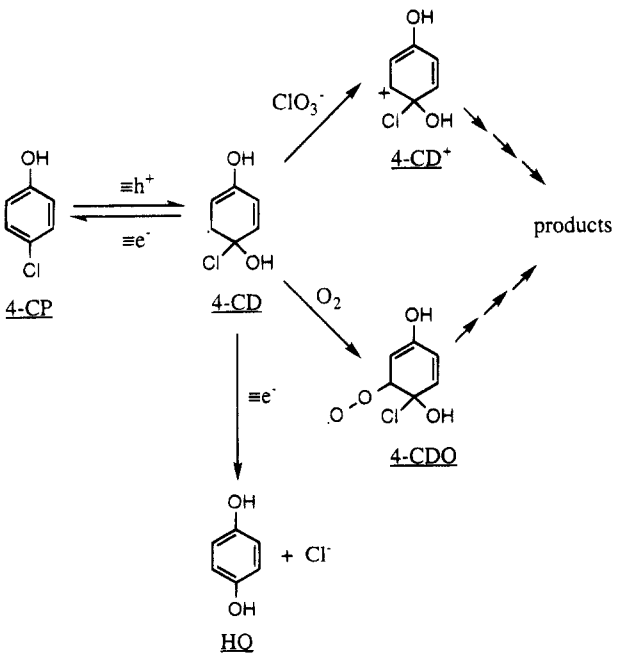

FIGURE 4. Reaction mechanism.

O_2), $\equiv ClO_3^-$ is adsorbed chlorate (e.g., $\equiv$Ti(IV)$OClO_2^-$), 4-CP is 4-chlorophenol, 4-CD is the 4-chlorodihydroxycyclodienyl radical, 4-CD^+ is the 4-chlorodihydroxycyclodienyl cation, $[\equiv \text{Ti(IV)}]_0$ is the concentration of $\equiv$Ti(IV) without adsorption.

We make several assumptions as follows:

(1) The reactions are not mass-transfer limited.

(2) Adsorption and desorption of all species is fast with respect to reaction rates, and the surface coverage may be described by a Langmuir–Hinshelwood adsorption isotherm (*38–41*).

(3) Double-layer and surface charge effects are negligible with respect to the kinetic analysis.

(4) 4-CP, O_2, and ClO_3^- compete for surficial Ti(IV) sites.

(5) Reactions take place between surface-adsorbedspecies (Table 2).

(6) The hydroquinone pathway (Figure 4) is not relevant to the kinetic description of the effects of O_2 and ClO_3^- on the oxidation of 4-CP.

The derivation begins by invoking charge neutrality (eq T2.23) and the steady-state approximation (eq T2.22) to write eqs T2.20–21 as follows:

$$[\equiv e^-] - [\equiv h^+] = k_5\left(\frac{1}{k_6} - \frac{1}{k_7}\right) \quad (9)$$

Equation 9 simplifies to eq 10 when holes and electrons are localized at the same rate (i.e., $k_6 = k_7$):

$$[\equiv e^-] = [\equiv h^+] \quad (10)$$

The chemical reactions (eqs T2.5–8) shown in Table 2 and the approximation that $k_6 = k_7$ are not a complete representation of the charge-carrier dynamics; however, the essential elements are included (*12, 13*).

Applying the steady-state approximation (eq T2.22) to eq T2.19 and substituting eq 10 into the resulting expression, we can write:

$$0 = -k_4[\equiv h^+]^2 - k_1[\equiv h^+][\equiv 4\text{-CP}] + k_5 \quad (11)$$

Solving eq 11 for $[\equiv h^+]$ at low quantum efficiencies (i.e., $k_1[\equiv h^+][\equiv 4\text{-CP}] \ll k_4[\equiv h^+]^2$) yields the following equation:

$$[\equiv h^+] = \sqrt{k_5/k_4} \quad (12)$$

Application of the steady-state approximation to eq T2.17 yields

$$[\equiv 4\text{-CD}] = \left(\frac{k_1[\equiv h^+][\equiv 4\text{CP}]}{k_{-1}[\equiv e^-] + k_2[\equiv ClO_3^-] + k_3[\equiv O_2]}\right) \quad (13)$$

Substituting eqs 10, 12, 13, Γ_1, Γ_2, and Γ_3 into eq T2.16 yields the following general equation for Φ the presence of both O_2 and ClO_3^-:

$$\Phi = \frac{d[4CP]/dt}{k_5} = \{k_1K_3[\equiv Ti(IV)]^2[4CP](k_2K_2[ClO_3^-] + k_3K_1[O_2])\}/\{k_{-1}k_5(1 + K_1[O_2] + K_2[ClO_3^-] + K_3[4CP])^2 + \sqrt{k_4k_5}[\equiv Ti(IV)](1 + K_1[O_2] + K_2[ClO_3^-] + K_3[4CP])(k_2K_2[ClO_3^-] + k_3K_1[O_2])\} \quad (14)$$

Under our experimental conditions, $KC(4\text{-CP}) = 0.013$ ($C = 100\ \mu M$ and $K = 1.3 \times 10^2\ M^{-1}$) (*11*). Two estimates of $KC(O_2)$ based upon kinetic measurements (*11, 42*) are 4.4 ($P = 1$ atm and $K = 4.4\ atm^{-1}$) (*11*) and 130 ($C = 1$ mM and $K = 1.3 \times 10^5\ M^{-1}$) (*43*). FTIR ATR measurements in our laboratory set an upper limit of $K(ClO_3^-) \ll 100\ M^{-1}$. If $K(ClO_3^-) \approx 10\ M^{-1}$, then KC varies from 1 to 10 for 0.1–1 M ClO_3^-, which is consistent with the kinetic observations in Figure 1 based upon a competition between O_2 and ClO_3^- for a common surface site (i.e., eq 14).

Special Cases. (1) Chlorate. When $[ClO_3^-] \gg [O_2]$ and [4-CP] is low, eq 14 is written as follows:

$$\Phi = \{k_1k_2K_2K_3[\equiv Ti(IV)]^2[4CP][ClO_3^-]\}/\{k_{-1}k_5(1 + K_2[ClO_3^-])^2 + \sqrt{k_4k_5}k_2K_2[\equiv Ti(IV)][ClO_3^-](1 + K_2[ClO_3^-])\} \quad (15)$$

To evaluate the effect of $\Delta[ClO_3^-]$, we consider $\partial\Phi/\partial[ClO_3^-]$ as follows:

$$\frac{\partial\Phi}{\partial[ClO_3^-]} = \{k_1k_{-1}k_2k_5K_2K_3[\equiv Ti(IV)]^2[4CP](1 - (k_{-1}k_5 + \sqrt{k_4k_5}k_2[\equiv Ti(IV)])K_2^2[ClO_3^-]^2/(k_{-1}k_5)\}/\{[k_{-1}k_5(1 + K_2[ClO_3^-])^2 + \sqrt{k_4k_5}k_2K_2[\equiv Ti(IV)][ClO_3^-]\times(1 + K_2[ClO_3^-])]^2\} \quad (16)$$

Thus, under high light intensity, $\partial\Phi/\partial[ClO_3^-] > 0$ when $[ClO_3^-] < K_2^{-1}$ as shown in eq 17:

$$[ClO_3^-] < [k_{-1}k_5/K_2^2(k_{-1}k_5 + \sqrt{k_4k_5}k_2[\equiv Ti(IV)])]^{1/2} \approx \frac{1}{K_2} \quad (17)$$

Hence, increasing $[ClO_3^-]$ at high light intensities increases Φ when [4-CP] is low and $[ClO_3^-] \gg [O_2]$. This behavior is shown in Figure 1. In addition, eq 17 predicts that at a sufficiently high $[ClO_3^-]$ (i.e., $[ClO_3^-] = K_2^{-1}$), $\Delta[ClO_3^-]$ should yield a decrease in Φ. The chemical interpretation is as follows: increasing $[ClO_3^-]$ favors the degradation pathway shown in Figure 4 (eq T2.3) but disfavors the pre-equilibria step (eq T2.15) by saturating the surface.

(2) Light Intensity. In consideration of light intensity, there are three regions included in our model. At high light intensities (i.e., k_5 is large), the second term in the denominator of eq 14 is negligible. In this case, Φ depends on the light intensity, I, as $\phi \propto I^{-1}$ and falls as the inverse of light intensity. At intermediate light intensities, the first term in the denominator is negligible, and Φ falls as $I^{-1/2}$. We have previously reported the functional form of $\Phi(I)$ (*12, 43, 44*). The linear relation between quantum efficiency and light intensity shown in Figure 3 indicates that our experiments were conducted in the region of high light intensity approaching the limit $\Phi \propto I^{-1}$. At low light intensities, eq 12 fails because high quantum efficiencies are obtained.

(3) Oxygen. When $[O_2] \gg [ClO_3^-]$ and [4-CP] is low, analogues to eqs 15–17 result due to the symmetry of eq 16 with respect to O_2 and ClO_3^-. Hence, at high light intensities, increased $[O_2]$ yields increase in Φ when [4-CP] is low and $[O_2] \gg [ClO_3^-]$. This behavior has been observed previously (*11*).

(4) 4-Chlorophenol. When $[O_2] \gg [ClO_3^-]$ and [4-CP] is high, eq 14 is written as follows:

$$\Phi = \{k_1k_3K_1K_3[\equiv Ti(IV)]^2[4CP][O_2]\}/\{k_{-1}k_5(1 + 2K_3[4CP] + (K_3[4CP])^2) + \sqrt{k_4k_5}k_3K_1[\equiv Ti(IV)](1 + K_3[4CP])[O_2]\} \quad (18)$$

The saturation effect of [4-CP] has been investigated previously and obeys a Langmuir–Hinshelwood isotherm (*11*). Equation 18 reduces to the L-H form when $k_0 = k_1[\equiv Ti(IV)]\sqrt{1/k_4k_5}$ and $K = K_3$ at a fixed intermediate light intensity (i.e., the second term in the denominator of eq 18 dominates).

(5) Chlorate and Oxygen. To understand the effects when both ClO_3^- and O_2 are present, we consider $\partial\Phi/\partial[ClO_3^-]$ of eq 14 at high $[O_2]$, low [4-CP], and high light intensity:

$$\frac{\partial\Phi}{\partial[ClO_3^-]} = k_1K_2K_3[\equiv Ti(IV)]^2[4\text{-CP}](-k_2K_2[ClO_3^-] + (k_2 - 2k_3)K_1[O_2])/k_5k_{-1}(K_1[O_2] + K_2[ClO_3^-])^3 \quad (19)$$

The sign of eq 19 is thus determined by the following expression:

$$-k_2K_2[ClO_3^-] + (k_2 - 2k_3)K_1[O_2] \quad (20)$$

This expression is negative since $k_3 > k_2$ (eq T2.24). Hence, an increase in $[ClO_3^-]$ yields a decrease in Φ. The behavior is shown in Figure 1a for low [4-CP], high $[O_2]$, and high light intensity.

The result embodied in eq 20 may seem initially counterintuitive. Figure 4 shows parallel pathways (eqs T2.3–4) so that increases in $[ClO_3^-]$ and $[O_2]$ would be expected to both yield enhanced degradation rates. However, the surface of TiO_2 is saturated with respect to O_2

under our experimental conditions. As a result, ClO_3^- displaces O_2. The loss of O_2, which has a higher reactivity than ClO_3^-, decreases Φ.

Iodide Oxidation. In order to test our proposed mechanism, several experiments were carried out with I^- as the primary electron donor. The oxidation pathway of I^- does not provide a reaction pathway with ClO_3^- (*vide infra*). Hence, the equivalent of eq T2.3 has a reaction rate constant $k_2 = 0$. The validity of the proposed mechanism is thus tested by the effect of $[ClO_3^-]$ on the oxidation rate of I^-, as discussed below.

The overall oxidation of I^- is a two-electron process as follows (*22, 29, 45–47*):

$$2I^- \leftrightarrow I_2 + 2e^- \qquad E^\circ = -0.620\ V \tag{21}$$

However, under normal experimental conditions, I_2 is rapidly complexed by I^- to form I_3^-:

$$I^- + I_2 \leftrightarrow I_3^- \qquad K = 770\ M^{-1},\ k_f = 5.6 \times 10^9\ M^{-1}\ s^{-1} \tag{22}$$

A likely reaction pathway initiated by valence-band hole oxidation is as follows:

$$I^- \leftrightarrow I^\bullet + e^- \qquad E^\circ = -1.3\ V \tag{23}$$

$$I^\bullet + I^- \rightarrow I_2^{\bullet-} \qquad K = 1.1 \times 10^5\ M^{-1},\ k = 1 \times 10^{10}\ M^{-1}\ s^{-1} \tag{24}$$

$$I_2^{\bullet-} \leftrightarrow I_2 + e^- \qquad E^\circ = -0.2\ V \tag{25}$$

Pathways due to oxidation by a surficial hydroxyl radical are also possible:

$$I^- + {}^\bullet OH_s \rightarrow I^\bullet + OH_s^- \qquad k = 1.2 \times 10^{10}\ M^{-1}\ s^{-1} \tag{26}$$

$${}^\bullet OH_s + I_2 \rightarrow HOI + I^\bullet \qquad k = 1.1 \times 10^{10}\ M^{-1}\ s^{-1} \tag{27}$$

$$I^\bullet + I^- \rightarrow I_2^{\bullet-} \qquad K = 1.1 \times 10^5\ M^{-1},\ k = 1 \times 10^{10}\ M^{-1}\ s^{-1} \tag{28}$$

The important iodine radicals believed to be present in the $KI/TiO_2/h\nu$ system are thus $I^\bullet$ and $I_2^{-\bullet}$. Although $I^\bullet$ is a potential oxidant (eq 23), its reaction with ClO_3^- is thermodynamically unfavorable ($E^\circ(ClO_3/ClO_3^-) \approx 2.1$ V) (*31*). The reduction of ClO_3^- by $I_2^{\bullet-}$ is considered to be of minor importance due to electrostatic repulsion of the reactants. Hence, in a heterogeneous $KI/TiO_2/h\nu/ClO_3^-$ system, no indirect oxidation pathway similar to the ClO_3^- pathway for 4-CP (Figure 4 and eq T2.3) is available.

Iodide–Kinetic Equations. The oxidation of I^- is described by equations similar to those in Table 2 with the following changes: $[\equiv I^-]$ is substituted for $[\equiv$4-CP$]$, $[\equiv I^\bullet]$ for $[\equiv$4-CD$]$, and $k_2 = k_3 = 0$. Employing eq 10, we write the quantum efficiency for the oxidation of iodide, Φ', as follows:

$$\Phi' = -(1/k_5)(d[I^-]/dt) = +k_1\sqrt{1/k_5k_4}[\equiv I^-] - k_{-1}\sqrt{1/k_5k_4}[\equiv I^\bullet] \tag{29}$$

We assume the time constant for steady-state concentrations of $I^\bullet$ and I_3^- is 10 min based upon the negative feedback with respect to I^- oxidation (Figure 3). An expression for the initial quantum efficiency for the oxidation (i.e., $t < 10$ min) of I^- is obtained by substituting $[\equiv I^\bullet] = 0$, Γ_1, Γ_2, and Γ_3 into eq 29 as follows:

$$\Phi' = k_1\sqrt{\frac{1}{k_5k_4}}\left(\frac{K_3[\equiv Ti(IV)][I^-]}{1 + K_1[O_2] + K_2[ClO_3^-] + K_3[I^-]}\right) \tag{30}$$

The initial quantum efficiency, Φ_i, for the formation of I_3^- (i.e., the oxidation product of I^-) is thus written as follows:

$$\Phi_i = \Phi' \tag{31}$$

The value of $KC(I^-)$ is 0.32 for $C = 1$ mM and $K = 3.2 \times 10^2$ M^{-1} (*18*). We would thus predict that Φ_i should decrease 10-fold upon the addition of either 1 mM O_2 or 0.1 M ClO_3^- because $KC(O_2) \approx 10$ and $KC(ClO_3^-) \approx 1$ are greater than $KC(I^- \approx 0.3)$. In fact, Φ_i varies in the range $(4.3–7.6) \times 10^{-4}$ (Figure 3). The competitive adsorption site model given by eq 31 thus does not describe heterogeneous oxidation of iodide.

When I^- binds noncompetitively to the surface of TiO_2 (i.e., a two-site model for I^-, on the one hand, and O_2 and ClO_3^-, on the other hand), the oxidation of I^- is described by the following equation (*18*):

$$\Phi_i = k_1\sqrt{\frac{1}{k_4k_5}}\left(\frac{K_3[\equiv Ti(IV)_A][I^-]}{1 + K_3[I^-]}\right) \tag{32}$$

based upon eq 31 for $K_1 = K_2 = 0$. In this case, I^- adsorbs to $\equiv Ti(IV)_A$ whereas O_2 and ClO_3^- adsorb to $\equiv Ti(IV)_B$. The addition of ClO_3^- thus does not affect the oxidation of I^-. In oxygenated solutions, conduction-band electrons are scavenged by O_2, which reduces charge-pair recombination. This effect may be included in eq 32 by reducing k_4 and thus increasing Φ_i. Finally, the addition of ClO_3^- to an oxygenated solution reduces $[\equiv O_2]$ via competitive adsorption for $\equiv Ti(IV)_B$, increases k_4, and thus decreases Φ_i. These predictions are confirmed by the results shown in Figure 3.

Under steady-state conditions (i.e., $t >$ 10 min), $[\equiv I^\bullet]$ can be written as follows (cf. eq 13):

$$[\equiv I^\bullet] = \left(\frac{k_1[\equiv h^+][\equiv I^-]}{k_{-1}[\equiv e^-]}\right) \tag{33}$$

Substitution of eq 10 into eq 33 and the resulting expression into eq 29 yields an expression for the steady-state oxidation of I^- as follows: $d[I^-]/dt = 0$. The I^-/I_3^- couple thus serves to introduce an additional charge-pair recombination pathway. However, although Φ_{ss} is less than Φ_i, Φ_{ss} is not zero (Figure 3). The cumulative oxidation of I^- may be explained by the concurrent irreversible oxidation of H_2O to produce $^\bullet OH$, which subsequently oxidizes I^-.

The purpose of the experiments with I^- was to test the validity of the mechanism proposed in Figure 4 and Table 2. Indeed, the kinetic behavior (eqs 32 and 33) of the oxidation of I^- in the presence of ClO_3^- is consistent with the proposed role of ClO_3^- in the oxidation of 4-CP (Figure 3).

Conclusions

Normal approaches to enhanced photoefficiencies of the TiO_2/UV process include reduction of the rate of charge-carrier recombination and enhancement of the rate of the primary interfacial charge transfer (*1, 12–14*). In line with

this approach, our results suggest that BrO_3^- scavenges conduction-band electrons, reduces charge-carrier recombination, and increases photoreactivity. At similar concentrations, BrO_3^- scavenges e^-_{cb} more efficiently than O_2. The reduced brominated products (e.g., BrO_2) may directly oxidize 4-CP and its products and may further scavenge e^-_{cb}. In this case, one photon yields several oxidative steps.

In contrast to BrO_3^-, ClO_3^- does not scavenge conduction-band electrons. Competitive adsorption occurs among 4-CP, ClO_3^-, and O_2 for surficial Ti(IV) sites, and the degradation of 4-CP follows three concurrent pathways. The proposed mechanism is shown in Figure 4 and Table 2, and the general kinetic equation is given in eq 14. The equation conforms to the dependency of rate of degradation of 4-CP on the concentrations of 4-CP, ClO_3^-, and O_2 and on the light intensity. The kinetics of the oxidation of I^- verify the proposed role of ClO_3^- as an oxidant of 4-CD.

In addition to scavenging e^-_{cb}, the oxyanions BrO_3^-, IO_4^-, and ClO_2^- may select reaction pathways via thermal oxidation. Higher quantum efficiencies should result when these oxyanions direct oxidation along efficient pathways for which multiple thermal oxidative events occur subsequent to photoinitiation. The obvious implication for heterogeneous photochemistry is that pathway-specific electron acceptors may provide effective routes to obtain higher quantum efficiencies. Furthermore, we note that macroscopic measurements of quantum efficiencies based upon product yields alone may not be representative of the branching ratio between charge-carrier recombination and interfacial charge transfer due to thermal oxidation steps.

Acknowledgments

We are grateful to ARPA and ONR {NAV 5 HFMN N0001492J1901} for financial support. Drs. Ira Skurnick and Harold Gund provided generous support and encouragement. S.T.M. is supported by a National Defense Science and Engineering Graduate Fellowship. A.T.L. is the recipient of a Summer Undergraduate Research Fellowship from Caltech. Wonyong Choi, Peter Green, Nicole Peill, and Janet Kesselman provided valuable support and stimulating discussion.

Literature Cited

(1) Hoffmann, M. R.; Martin, S. T.; Choi, W.; Bahnemann, D. W. *Chem. Rev.* **1995**, *95*, 69.
(2) Pelizzetti, E.; Carlin, V.; Minero, C.; Grätzel, M. *New J. Chem.* **1991**, *15*, 351.
(3) Abdullah, M.; Low, G. K. C.; Matthews, R. W. *J. Phys. Chem.* **1990**, *94*, 6820.
(4) Grätzel, C. K.; Jirousek, M.; Grätzel, M. *J. Mol. Catal.* **1990**, *60*, 375.
(5) Al-Ekabi, H.; Butters, B.; Delany, D.; Ireland, J.; Lewis, N.; Powell, T.; Story, J. In *Photocatalytic Purification and Treatment of Water and Air*; Ollis, D. F., Al-Ekabi, H., Eds.; Elsevier: Amsterdam, 1993; p 321.
(6) Vinodgopal, K.; Stafford, U.; Gray, K. A.; Kamat, P. V. *J. Phys. Chem.* **1994**, *98*, 6797.
(7) Stafford, U.; Gray, K.; Kamat, P.; Varma, A. *Chem. Phys. Lett.* **1993**, *205*, 55.
(8) Hofstadler, K.; Bauer, R.; Novalic, S.; Heisler, G. *Environ. Sci. Technol.* **1994**, *28*, 670.
(9) Mills, A.; Morris, S. *J. Photochem. Photobiol. A: Chem.* **1993**, *71*, 285.
(10) Mills, A.; Morris, S.; Davies, R. *J. Photochem. Photobiol. A: Chem.* **1993**, *70*, 183.
(11) Mills, A.; Morris, S. *J. Photochem. Photobiol. A: Chem.* **1993**, *71*, 75.
(12) Martin, S. T.; Herrmann, H.; Choi, W.; Hoffmann, M. R. *J. Chem. Soc. Faraday Trans.* **1994**, *90*, 3315.
(13) Martin, S. T.; Herrmann, H.; Hoffmann, M. R. *J. Chem. Soc. Faraday Trans.* **1994**, *90*, 3323.
(14) Martin, S. T.; Morrison, C. L.; Hoffmann, M. R. *J. Phys. Chem.* **1994**, *98*, 13695.
(15) Kormann, C.; Bahnemann, D. W.; Hoffmann, M. R. *J. Phys. Chem.* **1988**, *92*, 5196.
(16) Lepore, G.; Langford, C. H.; Víchová, J.; Vlcek, A. *J. Photochem. Photobiol. A: Chem.* **1993**, *75*, 67.
(17) Fitzmaurice, D. J.; Frei, H. *Langmuir* **1991**, *7*, 1129.
(18) Herrmann, J.; Pichat, P. *J. Chem. Soc. Faraday 1* **1980**, *76*, 1138.
(19) Draper, R. B.; Fox, M. A. *Langmuir* **1990**, *6*, 1396.
(20) Suatoni, J. C.; Snyder, R. E.; Clark, R. O. *Anal. Chem.* **1961**, *33*, 1894.
(21) Standbury, D. M. *Adv. Inorg. Chem.* **1989**, *33*, 69.
(22) Wardman, P. *J. Phys. Chem. Ref. Data* **1989**, *18*, 1637.
(23) Bard, A. J. *Science* **1980**, *207*, 139.
(24) Grätzel, M. *Acc. Chem. Res.* **1981**, *14*, 376.
(25) Nozik, A. J. *Nature* **1975**, *257*, 383.
(26) Fujishima, A.; Honda, K. *Bull. Chem. Soc. Jpn.* **1971**, *44*, 1148.
(27) Fujishima, A.; Honda, K. *Nature* **1972**, *238*, 37.
(28) Sawyer, D. T. *Oxygen Chemistry*; Oxford University Press: New York, 1991.
(29) Buxton, G. V.; Greenstock, C. L.; Helman, W. P.; Ross, A. B. *J. Phys. Chem. Ref. Data* **1988**, *17*, 513.
(30) Bielski, B. H. J.; Cabelli, D. E.; Arudi, R. L.; Ross, A. B. *J. Phys. Chem. Ref. Data* **1985**, *14*, 1041.
(31) Domae, M.; Katsumara, Y.; Jiang, P. Y.; Nagaishi, R.; Hasegawa, C.; Ishigure, K.; Yoshida, Y. *J. Phys. Chem.* **1994**, *98*, 190.
(32) Serpone, N.; Lawless, D.; Terzian, R.; Meisel, D. In *Electrochemistry in Colloids and Dispersions*; Mackay, R. A., Texter, J., Eds.; VCH Publishers, Inc.: New York, 1992; pp 399–416.
(33) D'Oliveira, J. C.; Al-Sayyed, G.; Pichat, P. *Environ. Sci. Technol.* **1990**, *24*, 990.
(34) Al-Ekabi, H.; Serpone, N.; Pelizzetti, E.; Minero, C. *Langmuir* **1989**, *5*, 250.
(35) Minero, C.; Aliberti, C.; Pelizzetti, E.; Terzian, R.; Serpone, N. *Langmuir* **1991**, *7*, 928.
(36) Laidler, K. J. *Chemical Kinetics*, 3rd ed.; Harper Collins: New York, 1987.
(37) March, J. *Advanced Organic Chemistry*, 4th ed.; John Wiley & Sons: New York, 1992.
(38) Wachs, I. E.; Saleh, R. Y.; Chan, S. S.; Cherisch, C. C. *Appl. Catal.* **1985**, *15*, 339.
(39) White, M. G. *Heterogeneous Catalysis*; Prentice-Hall Inc.: Englewood Cliffs, NJ, 1990.
(40) Turchi, C. S.; Ollis, D. F. *J. Catalysis* **1990**, *122*, 178.
(41) Stumm, W. *Chemistry of the Solid-Water Interface*; John Wiley & Sons, Inc.: New York, 1992.
(42) Cunningham, J.; Al-Sayyed, G. *J. Chem. Soc. Faraday Trans.* **1990**, *86*, 3935.
(43) Kormann, C.; Bahnemann, D. W.; Hoffmann, M. R. *Environ. Sci. Technol.* **1991**, *25*, 494.
(44) Hoffman, A. J.; Carraway, E. R.; Hoffmann, M. R. *Environ. Sci. Technol.* **1994**, *28*, 776.
(45) Kotronarou, A. Chemical Effects of Ultrasound in Water. Ph.D. Thesis, California Institute of Technology, 1991.
(46) Neta, P.; Huie, R. E.; Ross, A. B. *J. Phys. Chem. Ref. Data* **1988**, *17*, 1027.
(47) Elliot, A. J. *Can. J. Chem.* **1992**, *70*, 1658.

Received for review February 7, 1995. Revised manuscript received June 1, 1995. Accepted July 6, 1995.[⊗]

ES950078T

[⊗] Abstract published in *Advance ACS Abstracts*, August 15, 1995.